To appear in the 2008 IFAC Workshop on Navigation,
Guidance and Control of Underwater Vehicles

Autonomous Underwater Multivehicle Control with Limited Communication: Theory and Experiment

Daniel J. Klein, * **Patrick K. Bettale,** ** **Benjamin I. Triplett,** *
Kristi A. Morgansen *

* *Department of Aeronautics and Astronautics, University of Washington, Box 352400, Seattle, WA 98195-2400 (email: djklein@u.washington.edu, triplett@u.washington.edu, morgansen@aa.washington.edu).*
** *Department of Electrical Engineering, University of Washington, Box 352500, Seattle, WA 98195-2500 (email: pkhall@u.washington.edu).*

Abstract: The work here addresses the task of coordinated control design and implementation for systems of free-moving autonomous underwater vehicles linked via underwater communication. By treating heading angle as oscillator phase, a Kuramoto model approach is used to construct controls that align or anti-align headings. To accommodate communication events occurring at finite times, the system dynamics are expressed in discrete time with communication events occurring at the update instances. In this framework, appropriate broadcast communication topologies can be evaluated. The methods are demonstrated here both in simulation and in experiment with the University of Washington autonomous underwater multivehicle system.

Keywords: Underwater vehicles, cooperative control, communication network, nonlinear systems.

1. INTRODUCTION

During the past several years, the use of groups of autonomous vehicles to perform coordinated and cooperative tasks has been receiving a growing amount of attention. A key feature of such multivehicle groups is that communication between moving vehicles has several dynamic properties. In particular, not all agents may be able to communicate with all others, data rates may be low (either by environment or by design), dropouts may occur, etc. The majority of the work that has been done with respect to such systems has primarily focused on theoretic results, and even when dynamic communication is considered, system models are generally assumed to be linear (Ren et al., 2005; Olfati-Saber and Murray, 2004; Hatano and Mesbahi, 2005). Implementations of results on experimental testbeds have been much more limited, particularly for underwater vehicles. In some cases, testbeds have been developed with tethered underwater vehicles, where communication can be provided across the tether. In other applications, vehicles do not use underwater communication, but are restricted to surface communication such as with Iridium modems in the Autonomous Ocean Sampling Network II (AOSNII) (Paley et al., 2008). For open water applications, particularly in salt water, acoustic modems (see e.g. (Freitag et al., 2005)) are generally the preferred technology, but the integration of such devices into vehicles is still in early stages (Howe et al., 2007). For initial testing and development, these devices are too high power to be used in small testing tanks due to multipath signals.

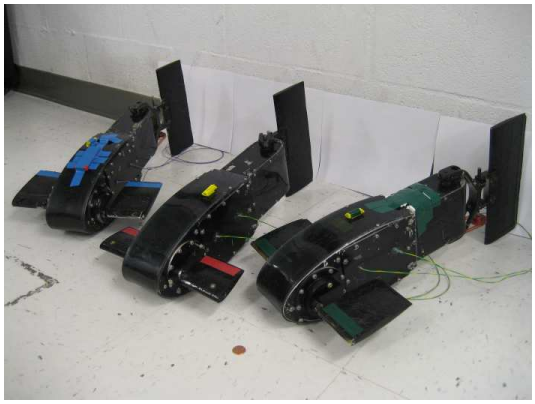

Fig. 1. UW autonomous fin-actuated underwater vehicles.

The primary contributions of the work in this paper are to extend results of the authors in coordinated heading control for nonlinear systems with dynamic communication and to examine the use of these results in implementation with the University of Washington Fin-actuated Autonomous Underwater System (UWMFAUS). To address the need for controlled development of coordinated control with wireless underwater communication, an RF transceiver has been built at the University of Washington for use in the UWMFAUS.

The remainder of the paper is organized as follows. In Sec. 2, the coordinated control task is presented with discussion. The physical characteristics of the system used to implement the control design is discussed in Sec. 3.

Experimental and simulation results are given in Sec. 4, with conclusions and future work discussed in Sec. 5.

2. COORDINATED CONTROL

A particular task of interest for underwater missions is coordinated target tracking. In target tracking tasks, one or more targets (e.g. whales, pollutants, etc) move in the environment, and the group task is to maintain sensor coverage of the target(s). To best leverage the multi-agent team, coordinated controllers have recently been designed to keep the spatial centroid of the team near the target position, thus permitting a diverse view of the target (Klein and Morgansen, 2006; Triplett et al., 2007).

A large number of underwater vehicles moving in the plane locomote via controlled forward/backward velocity and maneuver with heading control. The resulting nonlinear system can be crudely modeled with dynamics of the form

$$\frac{d}{dt}\begin{bmatrix} x \\ y \\ \theta \end{bmatrix} = \begin{bmatrix} v\cos(\theta) \\ v\sin(\theta) \\ u \end{bmatrix}. \tag{1}$$

These dynamics are generically referred to as a unicycle model and are applicable not only to underwater vehicles but also to many air and ground based systems.

Analytical results from (Klein and Morgansen, 2006) show that coordinated target tracking can be achieved for a group of N constant-speed planar unicycles (1) with a steering controller of the form

$$\dot{\theta}_i = u_i^{vm} + u_i^{sp}. \tag{2}$$

Here, u_i^{vm} is a term that drives the group centroid to the target vehicle. Meanwhile, u_i^{sp} acts to keep each vehicle near the group centroid. To begin, focus on the first term, which was inspired by the Kuramoto model of phase-coupled oscillator models that were first studied by Winfree (Winfree, 1967) and later by Kuramoto (Kuramoto, 1984) and Strogatz (Strogatz, 2000, 2003) as a tool for analyzing large groups of coupled phases. In the most generic form with all-to-all coupling, each vehicle heading has a single state variable θ_k, that evolves according to

$$\dot{\theta}_k = \omega_k + \frac{K}{N}\sum_{j=1}^{N}\sin(\theta_j - \theta_k). \tag{3}$$

Here, K is a gain, θ_k is the heading of the k^{th} vehicle, and ω_k is a fixed natural frequency. In the case of homogeneous natural frequencies ($\omega_k = \omega_0,\ \forall k$), ω_0 can be taken as zero without loss of generality by rewriting (3) in a rotating frame.

In the case of homogeneous natural frequencies, the behavior of the Kuramoto model (3) is dependent on the sign of the control gain. For $K > 0$, the model stabilizes to the aligned set,

$$\mathcal{A} = \{\theta \mid \|r(\theta)\| = 1\} \tag{4}$$

$$r(\theta) = \frac{1}{N}\sum_{i=1}^{N}\begin{bmatrix}\cos\theta_i \\ \sin\theta_i\end{bmatrix}, \tag{5}$$

in which all vehicles are pointed in the same direction. For $K < 0$, the Kuramoto model is stable to the balanced set,

$$\mathcal{B} = \{\theta \mid \|r(\theta)\| = 0\}, \tag{6}$$

in which the group headings are anti-aligned.

For a group of N constant-speed unicycles, the $\|r(\theta)\|$ is proportional to the velocity of the group centroid. Thus the Kuramoto model will drive the centroid velocity to a maximum value when $K > 0$ and to a minimum value of zero when $K < 0$. For target tracking, having the velocity of the group centroid match that of the target is desirable. To extend the Kuramoto model to target tracking, a reference velocity, v_{ref}, has been introduced (Klein and Morgansen, 2006),

$$\dot{\theta}_k = \frac{K}{N}\sum_{j=1}^{N}\sin(\theta_j - \theta_k) - Kv_{ref}^T\begin{bmatrix}-\sin(\theta_k) \\ \cos(\theta_k)\end{bmatrix}. \tag{7}$$

The result is that the velocity of the group centroid will approach the reference velocity.

While the above model is theoretically sound, each vehicle needs to know the heading of every other vehicle at every time instant. Clearly, this requirement is unreasonable when only limited communication is possible (i.e. underwater). This issue has been addressed (Triplett et al., 2005; Klein et al., 2008) by applying a zero order hold of length ΔT to the Kuramoto model in the case of homogeneous natural frequencies,

$$\theta_k(h+1) = \theta_k(h) + \frac{K\Delta T}{N}\sum_{j=1}^{N}\sin\left(\theta_j(h) - \theta_k(h)\right). \tag{8}$$

Recent research has integrated a reference velocity into this discretized Kuramoto model (Klein and Morgansen, 2008).

In an underwater setting, all-to-all communication is impractical due to inherent properties of the medium. In such settings, one can make an appeal for broadcast communication topologies in which one vehicle broadcasts to a subset of the other vehicles during each transmission session. With the broadcast communication topology, (8) can be rewritten as

$$\theta_k(h+1) = \begin{cases}\theta_k(h), & \text{if } k \text{ did not receive a new signal,} \\ \theta_k(h) + K\Delta T\sin(\theta_b(h) - \theta_k(h)), & \text{otherwise.}\end{cases} \tag{9}$$

Here, $\theta_b(h)$ is the heading of the broadcaster during step h. The order of the broadcaster sequence can have an impact on stability. Of theoretical importance is the case when each vehicle is equally likely to be selected as the broadcaster during any given transmission session. When the broadcaster is selected at random and all agents receive, the model is referred to as random one-to-all communication.

Theory indicates that this discretized model retains many of the desirable properties of the continuous-time Kuramoto model (3), while using significantly less communication. In particular, the stability to either aligned or balanced group states is dependent on the product of the coupling strength, K, and the time discretization, ΔT. The following characteristics are known about the discretized Kuramoto model:

(1) $0 < K\Delta T < 2$ is a sufficient condition for aligned set stability in the case of all-to-all or random one-to-all broadcast communications,
(2) $-1 < K\Delta T < 0$ is a sufficient condition for balanced set stability with all-to-all communication,

(3) $-2 < K\Delta T < 0$ is conjectured to be a sufficient condition for balanced set stability, again for all-to-all communication.

The following is a main theoretical contribution of this work.

Theorem 2.1. A necessary and sufficient condition for stability of the discrete-time Kuramoto model of phase coupled oscillators with identical natural frequencies to the aligned set is $0 < K\Delta T < 2$. This result holds for either all-to-all or random one-to-all communication topologies.

Proof: The sufficient condition has been presented in previous work, so the only point to be shown is that $0 < K\Delta T < 2$ is necessary. A necessary condition for an equilibrium point to be stable is that all eigenvalues of the linearized system matrix lie within the unit circle. Due to the rotational symmetry of the aligned set, the linearization can be done about the origin. In other words, the aligned set is stable if and only if the origin is stable.

Denote by B_c the incidence matrix associated with a complete graph on N nodes. The discrete-time Kuramoto model (8) can then be written as

$$\theta(h+1) = \theta(h) + \frac{K\Delta T}{N} B_c \sin(B_c^T \theta(h)). \tag{10}$$

Linearizing (10) about the origin yields

$$\theta(h+1) = A\theta(h) \tag{11}$$

$$A = \left(I - \frac{K\Delta T}{N} L_c \right), \tag{12}$$

where $L_c = B_c B_c^T$ is the graph Laplacian associated with the complete graph. The eigenvalues of A lie at

$$\lambda(A) = 1 - \frac{K\Delta T}{N} \lambda(L_c). \tag{13}$$

The eigenvalues of the graph Laplacian of an undirected complete graph are

$$\lambda(L_c) = \begin{cases} 0 & \text{with multiplicity one} \\ N & \text{with multiplicity } N-1. \end{cases} \tag{14}$$

All eigenvalues of A must lie within the unit circle for stability of the aligned set. Note that one eigenvalue will always be of value 1 (corresponding to $\lambda(L_c) = 0$) with eigenvector of all ones: $\mathbf{1}$. However, this eigenvalue/eigenvector pair corresponds to moving from point to point in the alignment subspace and has no effect on stability. For the remainder of the system, the dynamics are projected to a subspace orthogonal to $\mathbf{1}$. In this subspace, $0 < K\Delta T < 2$ is both necessary and sufficient for stabilization of the aligned set when connectivity is all-to-all. For the random one-to-all broadcast, the expected value of the next state given the current state evolves as in the all-to-all case. Thus, convergence is in probability. ■

Note that the balanced set, while stable for $-2 < K\Delta T < 0$ with all-to-all connectivity, is never stable with random one-to-all connectivity. Even if the state were to start balanced, as soon as one robot broadcasts to the others, the state would leave the balanced set. However, due to continuity, the state will not stray far from the balanced set for small values of $K\Delta T$. The system behavior in this case is the focus of experimental results presented below.

In the following section, two coordinated controllers based on the ideas and theory presented above will be designed and implemented on the underwater robots. Specifically, the tasks explored in the sequel are heading alignment and heading balancing using random one-to-all broadcast communications underwater. For the heading alignment task, one might consider a simple linear-consensus type protocol. However, the discrete-time Kuramoto controller is more appropriate because of the natural angle wrapping. Linear consensus was designed for linear spaces such as $\mathbb{R}^N$, not the N-Torus, $\mathbb{T}^N$, in which the set of N headings lies. This subtle difference creates some undesirable behavior of the linear consensus controller. For example, if one vehicle starts at 1° and a second vehicle at 359°, both vehicles will steer to meet at 180°. The Kuramoto controller is more natural in that the vehicles will meet near 0°, and this result extends to any number of vehicles.

3. HARDWARE DESCRIPTION

3.1 Autonomous Underwater Vehicles

The testbed used to implement the coordinated control methods in this work is the University of Washington Multivehicle Fin-actuated Autonomous Underwater System (UWMFAUS). The UWMFAUS is composed of three untethered autonomous underwater vehicles equipped with underwater communication (Sec. 3.3). The vehicles are operated an indoor freshwater tank instrumented with a four-camera tracking system for collecting data to supplement onboard vehicle sensing (Sec. 3.2).

Each of the three vehicles is completely self-contained with a servo-actuated two-link tail providing full motion control in the plane, and two independently servo-actuated "pectoral fin" bowplanes. Using both the tailfin and the pectoral fins, the vehicles have complete motion in 3D. Further, the vehicles can be fully operated with just the pectoral fins. In this mode, the vehicles can propel both forward and backward at slow speeds. Measuring approximately 0.5m in length and 3kg, the robots are each equipped with a microprocessor for collecting data and computing control commands, a pressure sensor for depth, a 3D compass, a radio-frequency transceiver, and NiMH rechargeable batteries. Full details of the construction and modeling of the individual vehicles can be found in (Morgansen et al., 2007).

3.2 Instrumented Testbed

The operation environment for the experiments presented below is a freshwater tank of dimensions 2.4m deep, 2.4m wide, and 6m long equipped with an external real-time vision system consisting of four identical underwater cameras connected to a central computer. Grayscale video frames are simultaneously captured from each camera at 30Hz. To maximize the available workspace, the cameras are mounted in the upper corners of the test tank, at a depth of approximately 5cm. Full details of the apparatus can be found in (Morgansen et al., 2007).

Simultaneous tracking of three underwater vehicles with the operational constraints and tracking equipment used here is a difficult and open research problem. To generate

the 3D tracking results for this paper, a separate particle filter is used for each robot with the assumption that the robots will not cross paths in all four camera views at the same time. Propagation is achieved using a Frenet-Serret model with variable speed and a zero order hold on control inputs. Because the estimator does not have access to the actual control inputs used by the robots, zero-mean Gaussian noise is assumed for each input. The observation model of the particle filter relies upon a Tsai camera calibration (Tsai, 1986, 1987) generated from known world to image point correspondences. This calibration allows each particle to be projected into each image, from which the likelihood is computed. Each camera is assumed to be independent, resampling is done after each update, and a total of 4000 particles are used per vehicle.

3.3 Short Range RF Underwater Communication

Underwater communication is made possible by a custom transceiver based on radio modules from Linx Technologies and designed to minimize the attenuating effects of the underwater medium. Specifically, a transmitter and receiver form a half-duplex switchable transceiver circuit, and an amplifier is used to extend the range of the transmitter module. The modules use a carrier frequency of 315 MHz and on-off keying (OOK). All communications between the robot processor and the transceiver board are asynchronous at 2400 baud through a transistor-transistor logic (TTL) serial link. Currently, the robots are communicating with full-wave and half-wave wire antennas mounted externally (see Fig. 1) to eliminate any radio loss incurred as a result of an air-water interface. The communication protocol currently implements a straight serial pass-through with Manchester (bi-phase) coding. A software state machine is used to continuously decode the output of the receiver, capturing any valid data and outputting it to the serial port.

These transceivers allow a single vehicle communicate with one or more other vehicles during each transmission session, depending on distance of the receiving vehicles from the transmitting vehicle. Thus, inter-vehicle communication can be modeled as a sequence of one-to-some logical broadcast graphs. Ideally, each broadcast would be received by all other robots so the each session would have a star topology, but in reality, not all transmissions are received by all vehicles.

4. EXPERIMENTS AND RESULTS

Experiments with three fin-actuated robots were conducted in the instrumented testbed to evaluate the performance of the coordinated controller in conjunction with random one-to-all broadcast communication. Two experiments, derived from the theory presented in Sec. 2, were run for this purpose. The first task for the controller was to drive all the robot headings to the aligned state, while the second task for the controller was to send the robot headings to the balanced state. Despite the apparent simplicity of the tasks, designing a controller that works in implementation on underwater vehicles is non-trivial due to the challenges of data transmission in the underwater environment. The results are quite promising, particularly given the high packet loss rate between 40% and 60%.

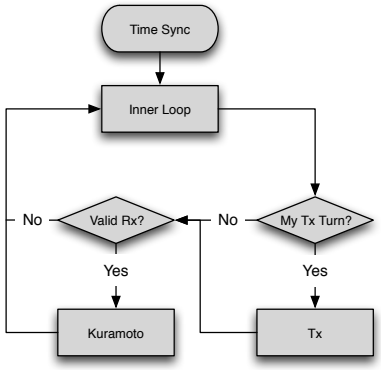

Fig. 2. Coordinated controller program flow block diagram.

For convenience, the three robots will be referred to as red, blue, and green in correspondence to markings on the individual robots. Because of the oscillatory nature of the robot motion from the tail-fin locomotion, heading data is averaged over a full tail period for feedback to the inner-loop heading control. To protect the robots against collisions, the blue, green, and red robots were respectively given depth setpoints of 0.3m, 0.6m, and 1.4m. Because the longitudinal and lateral dynamics are only loosely coupled, this choice has little impact on planar task performance.

The algorithm used for implementation of the vehicle coordinated control is shown in Fig. 2. Synchronized clocks were used to make the experiments match the theory as closely as possible. To achieve clock synchronization, before the robots are placed in the water, a base station sends out a sequence of 20 unique characters at a rate of one character per half-second. Upon reception of a character, the robot will pause until the time at which the last character in the sequence would be received. After pausing, all vehicles have synchronized clocks.

To realize a random one-to-all broadcast sequence, the robots use a pseudo-random number generator, seeded with zero. A robot will broadcast when the current random number modulus the number of robots matches the ID, which is zero for red, one for blue, and two for green.

When a robot is selected as the broadcaster, it transmits its heading using the radio-frequency communication devices. A simple encoding and decoding scheme is used to slightly compress the heading, which is a floating point value in degrees. The encoder maps the interval from [0,360) to the closest character in [0,255], using a linear transformation. The decoder similarly maps the received character in [0, 255] back to [0,360). To maximize the probability of a successful transmission, the encoded character is transmitted four times in quick succession. The transmission takes approximately 50ms to send. The receiving robots get this transmission approximately 10ms thereafter. Thus, the discrete time step in the controller, ΔT, has a firm lower bound.

4.1 Aligned Headings

For the heading alignment demonstration, the robots started at one end of the tank, with the red robot pointed down the length of the tank and the green and blue robots splayed approximately 65° to either side. The run time

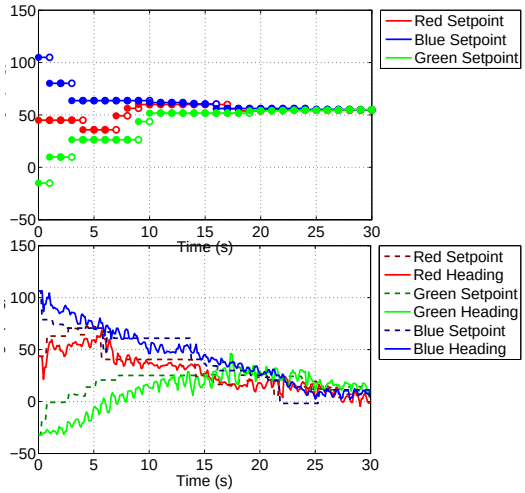

Fig. 3. Top: Simulation of three robots performing heading alignment with a 50% packet loss probability. Bottom: Experimental data of three robot heading alignment.

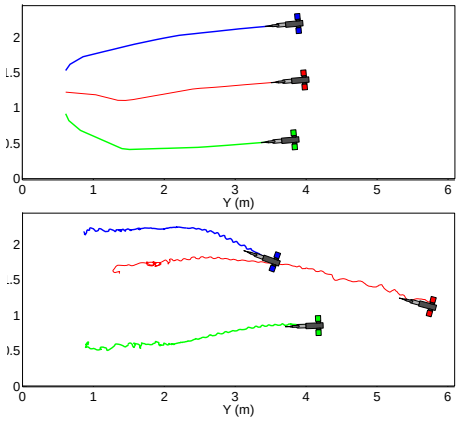

Fig. 4. Overhead view of the data from Fig. 3. Top: Simulation. Bottom: Experimental data of the x-y states of the three underwater vehicles as tracked by the camera system.

was set to 30s to prevent the robots from running into the far wall. The control gain was selected to be $K = 1$, and the time step was selected as $\Delta T = 0.5$s.

In addition to the physical experiment, a computer simulation was run using Matlab. The actual pseudo-random broadcast sequence used in the physical experiment was used in the simulation, however, drops were random. The main difference between the experiment and this simulation is that the simulation assumes a discretized planar kinematic unicycle model whereas the experiment is subject to the full dynamics of the underwater vehicles. The results from both the simulation and the experiment are shown in Figs. 3 and 4.

A key point concerning the experimental data is that the camera tracking system on the tank was not able to collect data for the first meter or so of the vehicle trajectories. Note that the initial segments of the green and blue robots shown in Fig. 4 does not correspond to movement from the initial heading of $\pm 65^o$ but from configurations that are close to alignment. These results demonstrate good heading alignment control considering experimental con-

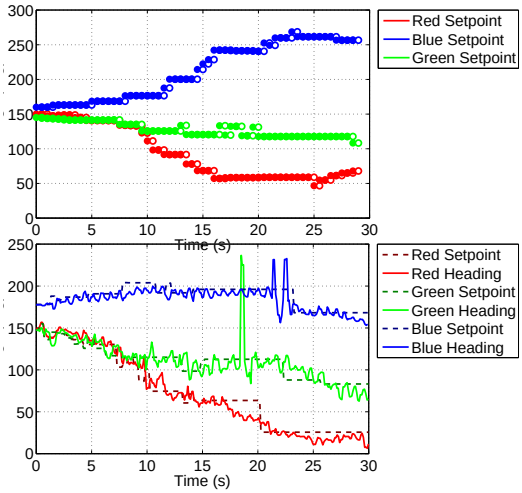

Fig. 5. Top: Simulation of three robots balancing headings with 50% packet loss. Bottom: Actual data from the robots.

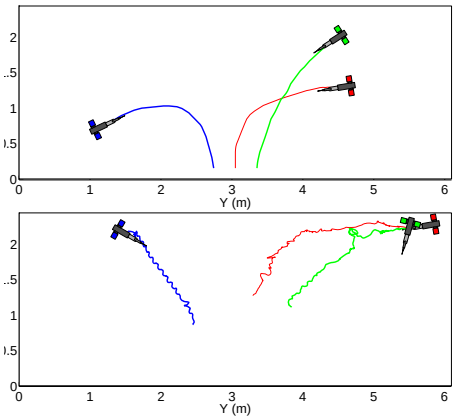

Fig. 6. Overhead view of the data from Fig. 5. Top: Simulation. Bottom: Experimental data of the x-y states of the three underwater vehicles as tracked by the camera system.

ditions that hinder the vehicle coordination. For example, magnetic fields from the building and the tank itself affect the readings of the compasses on board the robots. This magnetic field influence varies across the tank, and so affects the robots differently depending on their locations in the pool. This effect is clearly visible between the simulation and experimental results in Fig. 3 and Fig. 4 where the onboard experimental measurements indicate alignment, but the external tracking system indicates that the compass measurements have drifted.

4.2 Balanced Headings

For the balanced heading experiment, the initial position of the vehicles was at the side of the tank, halfway down its length. The initial heading of the red robot was parallel to the width of the tank, while the blue and green robots' initial headings were splayed $\pm 10°$, respectively, from that of the red robot. The runtime was set at 20s, and the time step was again selected as $\Delta T = 0.5$s. To make the group move toward the balanced state, the sign of the control gain was switched from the aligned heading experiment.

Further, to keep the vehicles as close as possible to a balanced group state with broadcast communication, the gain was selected as $K = -0.5$.

The balanced state heading experiment (Figs. 5 and 6) suffered the same challenges as the aligned heading experiment with environmental magnetic fields, communication reliability, and the size of the tank. However, the last two of these impediments to coordinated heading control were more problematic for the balanced state control than they were for the alignment control. The balanced heading control naturally drives the robots apart from one another, leading to greater separation between the radios, and the commensurate decrease in communication reliability. Also, the size of the pool is more constraining to the balanced state experiment. As can be seen in Fig. 6, both the red and blue robots encountered the far wall of the pool and were affected by it. While they were still able to control their headings when they encountered the pool wall, the heading control effectiveness of the robot tail mechanism is diminished by wall contact. Finally, note that in both simulation and experiment, the heading of the red vehicle crosses over that of the green vehicle. This crossing happened because red received from blue when green did not, and would not have occurred with all-to-all communication. Regardless, a near-balanced state is approached.

5. CONCLUSION

Overall, the experimental results are promising. Heading alignment and balancing did work, although the packet drop rate was greater than expected. Of particular interest was that the discrete time Kuramoto controller demonstrated robustness with respect to these delays, and future analytical work will be aimed at a mathematical investigation of this behavior.

Another positive result of this work is that the visual tracking system was able to simultaneously track three robots as they performed the coordinated maneuvers. Tracking multiple three-dimensional vehicles with numerous occlusions is not an easy task. While the position data looked good, estimates of roll, pitch, and yaw could still use some improvement which is the focus of ongoing work.

The transceivers did work successfully in the underwater environment. However, due to the large number of dropped packets, new radio hardware using a lower carried frequency will be designed and implemented. To further enhance data transmission, frequency shift keying (FSK) modulation will be used.

As these developments take place, more complicated coordination tasks will be tested and refined. In particular, one of the next tasks will be a demonstration of coordinated underwater target tracking.

ACKNOWLEDGEMENTS

The authors would like to thank Peter Reinhardt for assistance with experiments and data extraction.

This work was supported in part by the NSF under Grants CMS-0238461 and CCF-0728983 and in part by the AFOSR under Grants FA9550-05-1-0430 and FA9550-07-1-0528.

REFERENCES

Freitag, L., M. Grund, S. Singh, J. Partan, P. Koski, and K. Ball (2005). The WHOI micro-modem: An acoustic communications and navigation system for multiple platforms. In: *IEEE Oceans Conf.*

Hatano, Y. and M. Mesbahi (2005). Agreement over random networks. *IEEE Trans. Aut. Contr.,* **50**(11), pp. 1867–1872.

Howe, B.M., T. McGinnis, and M.L. Boyd (2007). Sensor network infrastructure: Moorings, mobile platforms and integrated acoustics. In: *Symp. Underwater Tech. and Workshop on Scientific Use of Submarine Cables and Related Technologies*.

Klein, D.J., P. Lee, K.A. Morgansen, and T. Javidi (2008, December). Integration of communication and control using discrete time Kuramoto models for multivehicle coordination over broadcast networks. *IEEE J. Selec. Areas Comm.,* **26**(4).

Klein, D.J. and K.A. Morgansen (2006). Controlled collective motion for trajectory tracking. In: *Proc. Amer. Contr. Conf.*

Klein, D.J. and K.A. Morgansen (2008). Set stability of phase-coupled agents in discrete time. In: *Proc. Amer. Contr. Conf.*

Kuramoto, Y. (1984). *Chemical Oscillations, Waves, and Turbulence*. Springer-Verlag, New York.

Morgansen, K.A., B.I. Triplett, and D.J. Klein (2007). Geometric methods for modeling and control of free-swimming fin-actuated underwater vehicles. *IEEE Trans. Robot.,* **23**(6), pp. 1184–1199.

Olfati-Saber, R. and R.M. Murray (2004). Consensus problems in networks of agents with switching topology and time-delays. *IEEE Trans. Aut. Contr.,* **49**(9), pp. 1520–1533.

Paley, D., F. Zhang, and N.E. Leonard (2008). Cooperative control for ocean sampling: The glider coordinated control system. *IEEE Trans. Contr. Sys. Techn*. Accepted for publication.

Ren, W., R.W. Beard, and E.M. Atkins (2005). A survey of consensus problems in multi-agent coordination. In: *Proc. Amer. Contr. Conf.*, pp. 1859–1864.

Strogatz, S.H. (2000). From Kuramoto to Crawford: exploring the onset of synchronization in populations of coupled oscillators. *Phys. D,* **143**, pp. 1–20.

Strogatz, S.H. (2003). *Sync: The Emerging Science of Spontaneous Order*. Hyperion Press.

Triplett, B.I., D.J. Klein, and K.A. Morgansen (2005). Discrete time kuramoto models with delay. In: *Networked Embedded Systems Conference*, pp. 9–23.

Triplett, B.I., D.J. Klein, and K.A. Morgansen (2007). Distributed estimation for coordinated target tracking in a cluttered environment. In: *ROBOCOMM*.

Tsai, R.Y. (1986). An efficient and accurate camera calibration technique for 3D machine vision. In: *IEEE Conf. Comp. Vision Pattern Recog.*

Tsai, R.Y. (1987). A versatile camera calibration technique for high-accuracy 3D machine vision metrology using off-the-shelf TV cameras and lenses. *IEEE Trans. Robot. Autom.,* **3**(4), pp. 323–344.

Winfree, A.T. (1967). Biological rhythms and behavior of populations of coupled oscillators. *J. Theor. Biol.,* **16**(1), pp. 15.